Biochemical and Biophysical Research Communications 460 (2015) 1063–1068

Contents lists available at ScienceDirect

Biochemical and Biophysical Research Communications

journal homepage: www.elsevier.com/locate/ybbrc

Major urinary protein 1 interacts with cannabinoid receptor type 1 in fatty acid-induced hepatic insulin resistance in a mouse hepatocyte model

Chin-Chang Chen [a], Tzung-Yan Lee [b], Ching-Fai Kwok [c], Yung-Pei Hsu [d], Kuang-Chung Shih [c], Yan-Jie Lin [a, d], Low-Tone Ho [a, c, d, e, *]

[a] Institute of Physiology, National Yang-Ming University, Taipei, Taiwan
[b] Graduate Institute of Traditional Chinese Medicine, Chang Gung University, Tao-Yuan, Taiwan
[c] Division of Endocrinology and Metabolism, Department of Medicine, Taipei Veterans General Hospital, Taipei, Taiwan
[d] Department of Medical Research, Taipei Veterans General Hospital, Taipei, Taiwan
[e] School of Medicine, National Yang-Ming University, Taipei, Taiwan

ARTICLE INFO

Article history:
Received 20 March 2015
Available online 3 April 2015

Keywords:
Major urinary protein 1
Cannabinoid receptor type 1
Hepatic insulin resistance
Mitochondrial dysfunction

ABSTRACT

Hepatic insulin resistance (HIR) is a metabolic abnormality characterized by increased gluconeogenesis which usually contributes from an elevation of free fatty acids. Cannabinoid receptor type 1 (CB1R) and major urinary protein 1 (MUP1) are thought to play pivotal roles in mitochondrial dysfunction, liver steatosis and insulin resistance. The aim of this study was to explore the role of MUP1 in CB1R-mediated HIR through the dysregulation of mitochondrial function in AML12 mouse hepatocytes challenged with high concentration of free fatty acids (HFFA). Firstly we observed that treatment of AM251, a selective CB1R antagonist, obviously reversed the HFFA-induced reduction of MUP1 protein expression both *in vivo* and *in vitro*. Additionally, our results revealed that AM251 also reverted HFFA-mediated decrease of the mRNA level of mitochondrial biogenesis-related factors, mtDNA amount, ATP production, mitochondrial respiratory complexes-I and -III, and mitochondrial membrane potential, thus consequently might correlate with a parallel reduction of ROS production. Meanwhile, AM251 attenuated HFFA-induced impairment of insulin signaling phosphorylation and elevation of phosphoenolpyrvate carboxykinase (PEPCK) and glucose 6-phosphatase (G6Pase), two key enzymes of gluconeogenesis. Silence of MUP1 gene abolished the inhibitory effect of AM251 on HFFA-mediated elevation of PEPCK and G6Pase expression, whereas the suppression of insulin signaling and mRNA level of mitochondrial biogenesis-related factors were only partially recovered. Altogether, these findings suggest that the anti-HIR effect of AM251 via improvement of mitochondrial functions might occur in a MUP1-dependent manner.

1. Introduction

Free fatty acids (FFAs) are the major link between obesity and insulin resistance [1], and contribute to the development of non-alcoholic fatty liver disease (NAFLD) [2]. The fasting hyperglycemia was observed in patients with type 2 diabetes (T2D) and metabolic syndrome resulted from reduced glucose uptake by peripheral tissues and increased production of glucose by hepatocytes resistant to insulin action. Insulin inhibits hepatic glucose production by inhibiting glucose formation from glycogenolysis and gluconeogenesis. Some metabolic data indicated that glycogenolytic flux is sensitively inhibited by physiological hyperinsulinemia, but gluconeogenic flux is not [3–5]. Thus, it is plausible that hepatic insulin resistance refers to impaired suppression of glucose production by insulin in hepatocytes via enhancement of gluconeogenesis. In eukaryotic cell, mitochondria are involved in energy production in the transfer of electrons and form of adenosine triphosphate (ATP). Amply evidence indicated that mitochondrial dysfunction is linked with T2D and age-related

* Corresponding author. Department of Medical Research, Taipei Veterans General Hospital, No.201, Sec. 2, Shipai Rd., Beitou District, Taipei City 11217, Taiwan. Fax: +886 2 28757634.
E-mail address: ltho@vghtpe.gov.tw (L.-T. Ho).

http://dx.doi.org/10.1016/j.bbrc.2015.03.155
0006-291X/

insulin resistance [6,7] and plays a key contributor in liver steatosis and steatohepatitis progression [8,9]. Overall, dysregulation of mitochondrial function arising from increased FFAs availability may play a pivotal role in hepatic steatosis causally contribution to insulin resistance.

The endocannabinoid system (ECS) consists of cannabinoid (CB) receptors, endocannabinoids and the enzymes involved in their biosynthesis and degradation, and has emerged as a role in the regulation of energy balance. It was reported that endogenous overactivation of peripheral CB1 receptor (CB1R) plays a vital mediator of insulin resistance and liver steatosis in experimental models of NAFLD [10,11]. Previous studies indicated that mechanisms by which hepatic CB1R signaling induces cyclic AMP-response element-binding protein H (CREBH)-mediated Lipin 1 gene expression, down-regulation of the insulin-degrading enzyme (IDE) and endoplasmic reticulum (ER) stress-dependent increase of ceramide synthesis contribute to suppress insulin receptor signaling and insulin clearance in liver, secondary to conduct insulin resistance *in vivo* model [12–14]. Additionally, Tedesco et al. suggested that CB1R stimulation impaired biogenesis and activity of mitochondria in the metabolic tissues of dietary obese mice [15].

Major urinary protein 1 (MUP1) is a lipocalin family member which is abundantly secreted into the circulation by the liver [16] and filtered by the kidneys into the urine and serves as a chemical communication, including volatile pheromones in adult male rodents [17,18]. In addition, MUP1 regulated nutrient metabolism independently of chemical signaling. It was reported that MUP1 expression was reduced in both genetic and high fat diet (HFD)-induced obese mice, and replenishment of recombinant MUP1 suppressed the expressions of both gluconeogenic and lipogenic genes in the liver and/or skeletal muscle in mice [19,20]. Meanwhile, Hui and coworkers suggested that MUP1-mediated improvement in glucose tolerance and insulin sensitivity may be attributed in part to enhancement of mitochondrial biogenesis and energy expenditure in skeletal muscle [20]. Our tissue proteomic analysis study showed that the MUP1 level was significantly decreased by 2.94-fold in the liver tissue of HFD mice compared with standard diet littermates, whereas treatment of HFD mice with AM251, a CB1R antagonist, nearly reversed the reduction (data in submission). Therefore, the present study intended to investigate the role of MUP1 in CB1R-mediated hepatic insulin resistance caused by FFAs, and to explore its mechanistic link with mitochondrial dysfunction related oxidative stress in AML12 mouse hepatocytes.

2. Materials and methods

2.1. Cell culture and in vitro treatment

AML12 mouse hepatocytes-derived cell line was obtained from the Food Industry Research and Development Institute (Hsinchu, Taiwan). AML12 cells were grown in a 1:1 mixture of DMEM/F12 culture medium (Gibco, NY, USA) containing 10% FBS, 5 μg/ml insulin, 5 μg/ml transferrin, 5 ng/ml selenium, and 40 ng/ml dexamethasone, and maintained at 37 °C in a humidified environment with 5% CO_2. For *in vitro* induction of insulin resistant state, high concentration of free fatty acids medium named HFFA medium was prepared according to method of Kohli [21] with minor modifications. In brief, HFFA medium was composed of 2:1 molar ratio of oleate/palmitate mixture in the pre-warmed culture medium (37 °C), followed by adding fatty acid-free BSA (at 5:1 molar ratio) and then gently mixed for 8 h at room temperature prior use.

2.2. Animals

Male C57BL/6 mice (3–4 week old) were purchased from the National Laboratory Animal Center (Taipei, Taiwan) and housed in a temperature- and light-controlled room (20 ± 2 °C; 12-h light/dark cycle). The mice were fed either a standard diet (STD; 13.5% calories from fat, LabDiet 5001, MO, USA) or a high-fat diet (HFD; 60% calories from fat, TestDiet 58G9, IN, USA) ad libitum for 12 weeks, followed by randomly dividing the HFD mice to receive once daily i.p. injections of the vehicle (7.7% DMSO, 4.6% Tween80, 87.7% saline) or 5 mg/kg body weight AM251, respectively, for 7 days. Finally, liver tissues of mice were exsanguinated under anesthesia and frozen immediately in liquid nitrogen and stored at −80 °C for analysis. An experimental protocol was approved by the Institutional Animal Care and Use Committee of Taipei Veterans General Hospital.

2.3. Immunohistochemistry stain and mitochondrial mass detection

For the MUP1 immunohistochemistry (IHC) stain, liver tissue slides were deparaffinized and hydrated with ethanol, then sequentially incubated in 0.3% H_2O_2 to block endogenous peroxidase activity, a specific anti-MUP1 antibody (R&D Systems, MN, USA) for 2 h at room temperature, and a biotinylated secondary antibody and avidin–biotin complex (ABC) reagent (Zymed Laboratories, CA, USA). Finally, color development was induced by DAB for 15 min and visualized under a light microscope. For mitochondrial mass assay, AML12 cells seeded onto glass coverslips were incubated with medium containing 100 nM Mitotracker red 580 (Invitrogen, Carlsbad, CA) for 30 min at 37 °C. Coverslips were rinsed with medium and PBS, then DAPI was used for nuclear staining. Finally, the cells were fixed in 4% paraformaldehyde for 15 min and visualized using fluorescence microscope.

2.4. Quantitative real-time PCR

Total RNA was extracted by using the guanidinium–phenol–-chloroform method, and the concentration and integrity of the isolated RNA were determined using OD 260/280. Total RNA (5 μg) was reverse-transcribed into cDNA by using the RevertAid™ First Strand cDNA Synthesis Kit (Thermo Scientific, MA, USA), followed by conducting real-time PCR using the SYBER system (Roche Applied Science, Mannheim, Germany) on a LightCycler 1.5 apparatus. PCR data were normalized to GAPDH expression as an internal control.

2.5. Immunoprecipitation and Western blotting

Cell lysates were extracted immediately using ice-cold lysis buffer containing 50 mM Tris–HCl (pH 7.4), 100 μM EDTA, 100 μM EGTA, 12 mM 2-mercaptoethanol, 1% phosphatase inhibitor cocktail 2 and protease inhibitor cocktail, followed by centrifugation at 13,000 × *g* for 30 min at 4 °C. Proteins were conjugated with anti-IRS-2 antibody for 1 h at 4 °C and immunoprecipitated using Protein G PLUS-Agarose (Santa Cruz, CA) with gentle shaking for 12 h at 4 °C. The cell lysates were separated using SDS-PAGE and transferred onto PVDF membranes. The membranes were blocked with blocking buffer containing 5% non-fat milk in TBS buffer for 1 h at room temperature. The signals were detected using an enhanced chemiluminescence kit (Millipore Corporation, MA, USA) and calibrated using β-actin as the internal control.

2.6. Mitochondrial DNA

The mitochondrial DNA copy number was determined using real-time PCR, as previously described by Tedesco et al. [22]. Briefly, genomic DNA was isolated by using the DNA extraction kit (Promega, WI, USA). PCR was conducted using the SYBER system on a LightCycler 1.5 apparatus. The ratio of mtDNA to nuclear DNA and mtDNA was reflected in the mitochondria concentration.

2.7. ATP and mitochondrial respiratory complexes content measurement

ATP content was measured with ATP bioluminescence assay kit HS II (Roche Applied Science) according to the manufacturer's protocol. Briefly, cells were lysed with lysis reagent and boiled at 100 °C for 10 min. The collected lysates were mixed with luciferase reagent and measured with Victor^{3}™ V multilabel counter (PerkinElmer, MA, USA). The luminescence value was normalized by protein concentration and ratio was adjusted with HFFA-free group. The mitochondrial fraction obtained by using mitochondrial isolation kit (Thermo Scientific), followed determined the mitochondria concentration using BCA method. The activity of the mitochondrial respiratory complex (MRC)-I and -III was analyzed as previously described [23].

2.8. Detection of reactive oxygen species and mitochondrial membrane potential using flow cytometry

For reactive oxygen species (ROS) assay, AML12 cells were incubated with 10 μM DCFH-DA reagent for 40 min at 37 °C before termination of treatment. Cells were washed and scraped gently with ice-cold PBS, then DCF fluorescence was detected according to the manufacturer's instructions (Invitrogen). The mean fluorescence intensity of JC-1 (BD™ MitoScreen Kit, BD Biosciences, CA) was measured to determine the mitochondrial membrane potential (MMP). Treated cells were collected and resuspended at a concentration of 1×10^5/ml in PBS which contained 1 μg/ml JC-1 and incubated for 30 min at 37 °C. Samples were analyzed by flow cytometry using a FACSCalibur (BD Biosciences). The data were calculated by fluorescence relative percentage.

2.9. MUP1 siRNA transient transfection

The MUP1 gene was silenced using siRNA according to the manufacturer's instructions (GE Dharmacon, Lafayette, USA). 5.0 nmol of a scramble control or siRNA of MUP1 (siMUP1 SMART pool) was added to sterilized, RNA-free water to stock a concentration of 100 μM. AML12 cells were transfected using DharmaFECT I transfection reagent combined with 100 nM MUP1 siRNA duplex in DMEM/F12 culture medium without antibiotics. After 60 h, cells were treated with the HFFA-medium and harvested by various experimental conditions.

2.10. Statistical analyses

Data are presented as mean ± S.E.M of at least 3 independent experiments. Comparisons among groups were performed using one-way analysis of variance (ANOVA) and Tukey's post hoc tests. Different letters indicated statistically significant difference ($p < 0.05$).

3. Results

3.1. Effect of AM251 on hepatic MUP1 level in HFD-fed mice

Results of liver IHC stain have shown a decrease in MUP1 level in HFD mice as compared with that of the STD-control mice (the arrow depicted the sites of MUP1), and this phenomenon was reversed by treating with 5 mg/kg AM251 in HFD mice (Fig. 1A). The parallel situation existed corresponding to MUP1 protein expression in the liver of HFD mice in the presence and absence of AM251 (Fig. 1B), although the MUP1 mRNA level did not represent a significant difference among these 3 groups (Fig. 1C).

3.2. AM251 treatment attenuated HFFA-induced mitochondrial dysfunction, ROS production and hepatic insulin resistance in AML12 cells

Our results indicated that the mitochondrial mass was decreased after challenge with 1 mM HFFA compared to that in HFFA-free medium. AM251 supplementation reverted HFFA-induced reduction of mitochondrial mass (Fig. 2A). The mRNA levels of peroxisome proliferator-activated receptor γ coactivator 1 α (PGC-1α), mitochondrial transcription factor A (TFAM), nuclear respiratory factor-1 (NRF-1) and NRF-2 were significantly decreased by 1 mM HFFA challenge, yet pre-treatment with AM251 attenuated HFFA-inhibited gene expression on the aforementioned regulators levels, especially in 1 and 3.3 μM AM251 (Fig. 2B). Furthermore, AM251 treatment obviously enhanced HFFA-suppressed mtDNA copy number and cellular ATP amount (Fig. 2C). The mitochondrial respiratory complexes consist of five

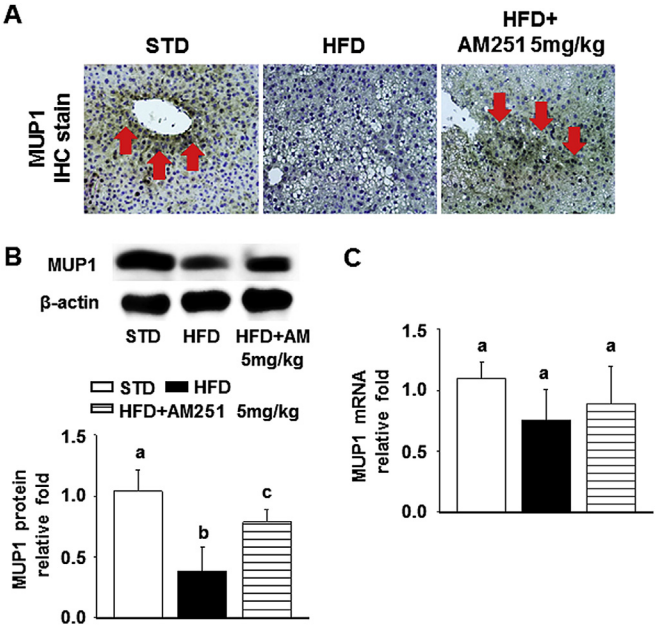

Fig. 1. Effect of AM251 on MUP1 expression of liver tissue in HFD-fed mice. (A) Liver tissues from STD-, HFD-, and HFD-fed mice treated with 5 mg/kg AM251 were obtained and fixed in 4% paraformaldehyde for MUP1 IHC stain. The indication of MUP1 was displayed as a dark brown color in the IHC stain (at the arrow sign). The results are shown at 200× magnification. (B) Protein and (C) mRNA levels of the MUP1 of liver tissues from STD-fed and HFD-fed mice with or without AM251 treatment were detected using real-time PCR and Western blotting, separately. The data are represented as the mean ± SEM for 3 independent measurements. (For interpretation of the references to colour in this figure legend, the reader is referred to the web version of this article.)

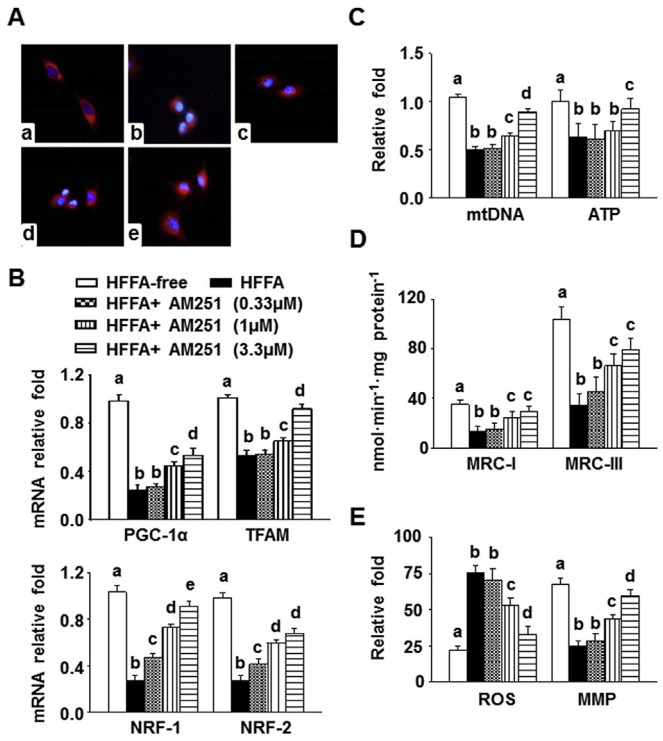

Fig. 2. AM251 attenuated HFFA-induced mitochondrial dysfunction in AML12 cell. AM251 was pre-treated for 2 h, subsequently co-incubated with AM251 plus 1 mM HFFA for various times (ROS production for 1 h, MMP for 8 h, ATP level for 24 h and other experiments for 12 h). (A) Mitochondrial mass was visualized as Mitotracker red signal by fluorescence microscopy. DAPI was used for nuclear staining. (a) HFFA-free; (b) HFFA; (c) HFFA+ 0.33 μM AM251; (d) HFFA+ 1 μM AM251; (e) HFFA+ 3.3 μM AM251, the results were shown at 200× magnification. (B) The mRNA levels of PGC-1α, TFAM, NRF-1 and NRF-2 were analyzed by real-time PCR. (C) The mtDNA amount was detected by real-time PCR and expressed as mtDNA copy number per nuclear DNA copy number. Relative cellular ATP level was analyzed and adjusted with HFFA-free condition. (D) MRC-I and -III activity were determined by spectrophotometrical activity assay. (E) Cellular ROS production and MMP were detected by flow cytometry against DCFH-DA and JC-1 fluorescence. The results are represented as the mean ± SEM for at least 3 experiments. (For interpretation of the references to colour in this figure legend, the reader is referred to the web version of this article.)

subunit complexes. MRC-I is the largest proton pump and MRC-III plays a critical role in biochemical generation of ATP. As shown in Fig. 2D, 1 mM HFFA treatment caused a marked decrease in MRC-I and -III activity, and AM251 prevented the HFFA-reduced these complexes. In addition, ROS expression by treatment with HFFA was much higher than HFFA-free medium, but had been significantly decreased after co-culture with AM251 (Fig. 2E). MMP level was greatly decreased upon treatment with HFFA, and AM251 treatment also prevented the HFFA-decreased MMP level (Fig. 2E). To further examine the role of CB1R in insulin resistance caused by HFFA challenge. The data showed that reduction of insulin receptor substrate-2 (IRS-2), PI3K and AKT phosphorylation levels after HFFA challenge was reversed by AM251 treatment (Supplementary Fig. 1). Phosphoenolpyrvate carboxykinase (PEPCK) and glucose 6-phosphatase (G6Pase), two key enzymes of gluconeogenesis were represented as indicators of hepatic insulin resistance [24]. Our results revealed that treatment of 1 mM HFFA reversed insulin suppression of cAMP/dexamethasome-mediated mRNA and protein levels of PEPCK and G6Pase, and these phenomena were abrogated by treating with AM251 (Supplementary Fig. 2). These results indicated that CB1R is involved in the development of HFFA-induced mitochondrial dysfunction and hepatic insulin resistance in AML12 cells.

3.3. Silence of MUP1 gene diminished the effect of AM251 on HFFA-mediated inhibition of insulin signaling, dysregulation of mitochondrial biogenesis and elevation of PEPCK and G6Pase levels in AML12 cells

To mimic reduction of hepatic MUP1 protein level as observed in our HFD-fed mice was upregulated by treating with 5 mg/kg AM251, HFFA-medium was used to investigate a series of mechanism between CB1R and MUP1 in AML12 cells. As shown in Fig. 3A, the suppression of MUP1 protein level in AML12 cells after treatment with 1 and 2 mM HFFA had a dose-responded effect. Meanwhile, 3.3 μM AM251 treatment prevented 1 mM HFFA-inhibited MUP1 protein expression (Fig. 3B). Subsequently, we applied siRNA against MUP1 to verify the direct correlation between CB1R and MUP1, which might cause dysregulation of mitochondrial biogenesis, inhibition of insulin signaling and alterations of PEPCK and G6Pase underlying the stimulation of HFFA. Our results showed that the protein level of MUP1 was reduced about 90% in AML12 cells after incubated with 100 nM siRNA against MUP1 (Fig. 3C). Pre-incubation with MUP1 siRNA diminished AM251-reversed suppression of IRS-2, PI3K and AKT phosphorylation which was incubated in 1 mM HFFA (Fig. 3D). The parallel situation existed corresponding to the mRNA levels of PGC-1α, TFAM, NRF-1 and NRF-2 in AML12 cells (Fig. 4A). Meanwhile, our results showed that genetic silence of MUP1 remarkably abolished the inhibitory effect of 3.3 μM AM251 on HFFA-induced PEPCK and G6Pase levels (Fig. 4B).

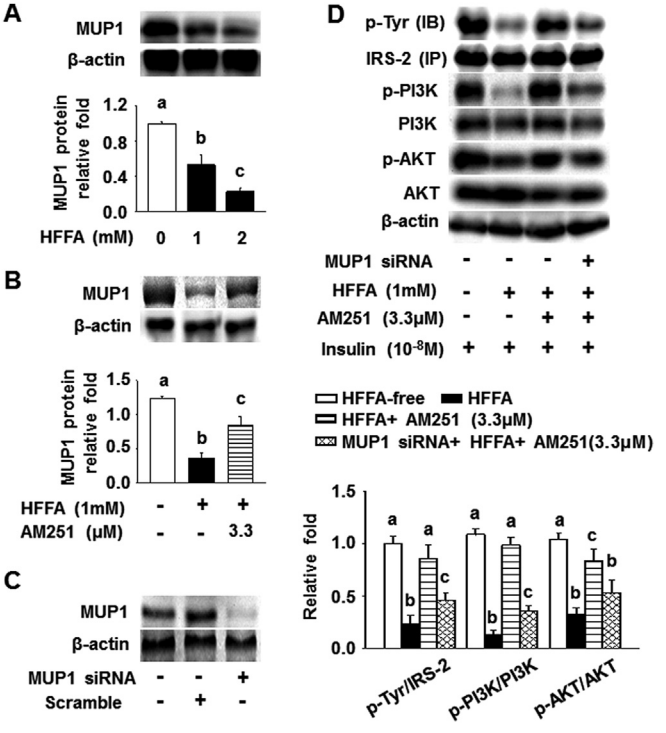

Fig. 3. Genetic ablation of MUP1 diminished the effect of AM251 on HFFA-inhibited insulin signaling phosphorylation in AML12 cell. (A) Protein level of the MUP1 was analyzed using Western blotting after challenge with 1 and 2 mM of HFFA for 6 h. (B) Protein level of MUP1 was detected after pre-treatment with 3.3 μM AM251 for 2 h, followed co-incubation with AM251 plus 1 mM HFFA for 6 h. (C) Alteration expression of MUP1 protein after the MUP1 siRNA was introduced into AML12 cells via transient transfection for 60 h. (D) Total and phosphorylated forms of IRS-2, PI3K and AKT in AML12 cells after sequential treatments with MUP1 siRNA, 3.3 μM AM251 for 2 h, AM251 plus 1 mM HFFA for 12 h and 10^{-8} M insulin for 30 min. The results are represented as the mean ± SEM for at least 3 experiments.

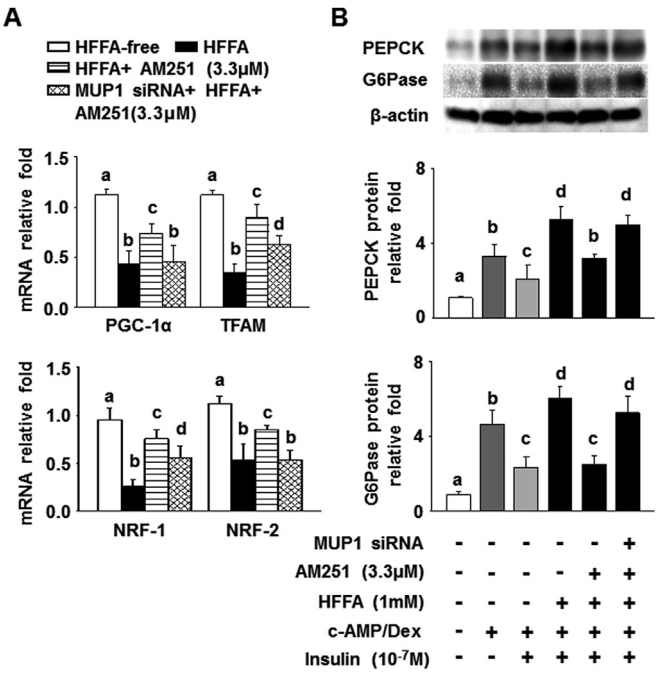

Fig. 4. Genetic ablation of MUP1 diminished the effect of AM251 on HFFA-induced dysregulation of mitochondrial biogenesis and abolished the elevation of PEPCK and G6Pase levels. (A) The mRNA levels of PGC-1α, TFAM, NRF-1 and NRF-2 were analyzed by real-time PCR after MUP1 gene ablation followed by exposure to pre-treat with 3.3 μM AM251 for 2 h and co-incubate with AM251 plus 1 mM HFFA for 12 h. (B) Protein levels of PEPCK and G6Psase in AML12 cells after sequential treatments with MUP1 siRNA, 3.3 μM AM251 for 2 h, AM251 plus 1 mM HFFA for 24 h, 10^{-7} M insulin for 30 min, and cAMP (100 μM)/dexamethasone (500 nM) (c-AMP/Dex) for 2 h. Results are expressed as the mean ± SEM for 3 experiments.

4. Discussion

Evidence indicated that mitochondrial dysfunction plays a central role in the pathogenesis of insulin resistance and NAFLD [9,25]. The present study demonstrated that pharmacological blockade of CB1R protected hepatocytes from HFFA-induced dysregulation of mitochondrial function and hepatic PEPCK and G6Pase levels via MUP1-dependnet manner. Emerging evidence suggested that the ECS modulates mitochondrial integrity and function. It was reported that exposure of cells and/or isolated mitochondria to endocannabinoid ligands displayed deleterious effects on oxygen consumption, MMP and ATP production [26,27]. In addition, reduction in PGC-1α also contributed to FFA-induced mitochondrial dysfunction and loss of insulin sensitivity in muscle cells [28]. Mitochondria contain nuclear-encoded proteins required for mtDNA maintenance including PGC-1α and TFAM; meanwhile, expressions of TFAM and several MRC polypeptides are controlled by NRF-1 and NRF-2.

Herein, we showed that AM251 markedly upregulated HFFA-suppressed mitochondrial mass, mitochondrial biogenesis, mtDNA amount and ATP production in AML12 hepatocytes. Previous studies showed the activity of MRC complexes was decreased in liver tissue from patients with NASH [29]. In addition, Vial et al. reported that high-fat diet feeding affects hepatocyte energy metabolism leading to depressed fatty acid β-oxidation and respiration as well as increased mitochondrial ROS production in spite of enhancement of MMP level in rats [30]. Correspondingly, AM251 treatment improved the activity of MRC-I, MRC-III and MMP levels in AML12 cells might positively correlate with suppression of ROS production.

Baur et al. suggested that resveratrol treatment markedly increased hepatic level of MUP1, PGC-1α and mitochondrial number, and further improved insulin sensitivity and reduced hyperglycemia in HFD-fed mice [31]. Likewise, PPARγ agonist rosiglitazone had been reported to partially reverse decreased level of MUP1 in liver tissue of *db*/*db* obese mice [20]. Herein, it has been observed that administration of AM251 reversed the decrease of hepatic MUP1 content in our HFD mice and HFFA-challenged hepatocytes models (see Figs. 1 and 4B). Furthermore, knockdown of MUP1 abrogated effectively the inhibitory effect of AM251 on HFFA-induced PEPCK and G6Pase levels in AML12 cells, whereas the suppression of insulin signaling was only partially recovered (see Fig. 3D). This finding was consistent with that MUP1 inhibited hepatic gluconeogenic program did not go fully through upregulation of insulin sensitivity in the liver of *db*/*db* mice as reported by Zhou et al. [19]. Therefore, the mechanism of MUP1 in regulation of PEPCK and G6Pase involves both insulin-dependent and insulin-independent pathways. The other way involves cAMP-related transcription signaling pathways, which are regulated by glucagon and catecholamine, etc, but this concept is required extensive experiment to proof in the future. Furthermore, Rector et al. suggested that hepatic mitochondrial dysfunction precedes the development of NAFLD and insulin resistance in the OLETF rats [25]. Since MUP1 silencing also neutralized the effects of AM251 on HFFA-inhibited gene expression of mitochondrial biogenesis, it is conceivable that MUP1 interacts with CB1R at mitochondria level in gluconeogenesis and insulin signaling, based on our evidence. Taken together, these findings highlight an important role of MUP1 in metabolic syndrome and broaden the scope of CB1R antagonism intervention.

Conflict of interest

There are no conflict of interest and no financial disclosure.

Acknowledgments

This work was supported by grants from the Taipei Veterans General Hospital, Taipei, Taiwan (V100C-072, L.T. Ho) and the Ministry of Science and Technology, Taipei, Taiwan (NSC 101-2320-B-182-017, T.Y. Lee).

Appendix A. Supplementary data

Supplementary data related to this article can be found at http://dx.doi.org/10.1016/j.bbrc.2015.03.155.

Transparency document

The Transparency document associated with this article can be found in the online version at http://dx.doi.org/10.1016/j.bbrc.2015.03.155.

References

[1] E. Maury, S.M. Brichard, Adipokine dysregulation, adipose tissue inflammation and metabolic syndrome, Mol. Cell. Endocrinol. 314 (2010) 1–16.
[2] S.H. Koo, Nonalcoholic fatty liver disease: molecular mechanisms for the hepatic steatosis, Clin. Mol. Hepatol. 19 (2013) 210–215.
[3] A. Adkins, R. Basu, M. Persson, et al., Higher insulin concentrations are required to suppress gluconeogenesis than glycogenolysis in nondiabetic humans, Diabetes 52 (2003) 2213–2220.
[4] G. Boden, P. Cheung, C. Homko, Effects of acute insulin excess and deficiency on gluconeogenesis and glycogenolysis in type 1 diabetes, Diabetes 52 (2003) 133–137.
[5] F.Q. Nuttall, A. Ngo, M.C. Gannon, Regulation of hepatic glucose production and the role of gluconeogenesis in humans: is the rate of gluconeogenesis constant? Diabetes Metab. Res. Rev. 24 (2008) 438–458.

[6] C.S. Stump, K.R. Short, M.L. Bigelow, et al., Effect of insulin on human skeletal muscle mitochondrial ATP production, protein synthesis, and mRNA transcripts, Proc. Natl. Acad. Sci. U. S. A. 100 (2003) 7996–8001.
[7] K.F. Petersen, D. Befroy, S. Dufour, et al., Mitochondrial dysfunction in the elderly: possible role in insulin resistance, Science 300 (2003) 1140–1142.
[8] D. Pessayre, B. Fromenty, A. Mansouri, Mitochondrial injury in steatohepatitis, Eur. J. Gastroenterol. Hepatol. 16 (2004) 1095–1105.
[9] D. Pessayre, B. Fromenty, NASH: a mitochondrial disease, J. Hepatol. 42 (2005) 928–940.
[10] D. Osei-Hyiaman, M. DePetrillo, P. Pacher, et al., Endocannabinoid activation at hepatic CB1 receptors stimulates fatty acid synthesis and contributes to diet-induced obesity, J. Clin. Invest. 115 (2005) 1298–1305.
[11] D. Osei-Hyiaman, J. Liu, L. Zhou, et al., Hepatic CB1 receptor is required for development of diet-induced steatosis, dyslipidemia, and insulin and leptin resistance in mice, J. Clin. Invest. 118 (2008) 3160–3169.
[12] D. Chanda, Y.H. Kim, D.K. Kim, et al., Activation of cannabinoid receptor type 1 (Cb1r) disrupts hepatic insulin receptor signaling via cyclic AMP-response element-binding protein H (Crebh)-mediated induction of Lipin1 gene, J. Biol. Chem. 287 (2012) 38041–38049.
[13] J. Liu, L. Zhou, K. Xiong, et al., Hepatic cannabinoid receptor-1 mediates diet-induced insulin resistance via inhibition of insulin signaling and clearance in mice, Gastroenterology 142 (2012) 1218–1228 e1211.
[14] R. Cinar, G. Godlewski, J. Liu, et al., Hepatic cannabinoid-1 receptors mediate diet-induced insulin resistance by increasing de novo synthesis of long-chain ceramides, Hepatology 59 (2014) 143–153.
[15] L. Tedesco, A. Valerio, M. Dossena, et al., Cannabinoid receptor stimulation impairs mitochondrial biogenesis in mouse white adipose tissue, muscle, and liver: the role of eNOS, p38 MAPK, and AMPK pathways, Diabetes 59 (2010) 2826–2836.
[16] F.G. Berger, P. Szoka, Biosynthesis of the major urinary proteins in mouse liver: a biochemical genetic study, Biochem. Genet. 19 (1981) 1261–1273.
[17] A. Cavaggioni, C. Mucignat-Caretta, Major urinary proteins, alpha(2U)-globulins and aphrodisin, Biochim. Biophys. Acta 1482 (2000) 218–228.
[18] J.L. Hurst, C.E. Payne, C.M. Nevison, et al., Individual recognition in mice mediated by major urinary proteins, Nature 414 (2001) 631–634.
[19] Y. Zhou, L. Jiang, L. Rui, Identification of MUP1 as a regulator for glucose and lipid metabolism in mice, J. Biol. Chem. 284 (2009) 11152–11159.
[20] X. Hui, W. Zhu, Y. Wang, et al., Major urinary protein-1 increases energy expenditure and improves glucose intolerance through enhancing mitochondrial function in skeletal muscle of diabetic mice, J. Biol. Chem. 284 (2009) 14050–14057.
[21] R. Kohli, X. Pan, P. Malladi, et al., Mitochondrial reactive oxygen species signal hepatocyte steatosis by regulating the phosphatidylinositol 3-kinase cell survival pathway, J. Biol. Chem. 282 (2007) 21327–21336.
[22] L. Tedesco, A. Valerio, C. Cervino, et al., Cannabinoid type 1 receptor blockade promotes mitochondrial biogenesis through endothelial nitric oxide synthase expression in white adipocytes, Diabetes 57 (2008) 2028–2036.
[23] M.A. Birch-Machin, D.M. Turnbull, Assaying mitochondrial respiratory complex activity in mitochondria isolated from human cells and tissues, Methods Cell Biol. 65 (2001) 97–117.
[24] N. Yabaluri, M.D. Bashyam, Hormonal regulation of gluconeogenic gene transcription in the liver, J. Biosci. 35 (2010) 473–484.
[25] R.S. Rector, J.P. Thyfault, G.M. Uptergrove, et al., Mitochondrial dysfunction precedes insulin resistance and hepatic steatosis and contributes to the natural history of non-alcoholic fatty liver disease in an obese rodent model, J. Hepatol. 52 (2010) 727–736.
[26] A. Athanasiou, A.B. Clarke, A.E. Turner, et al., Cannabinoid receptor agonists are mitochondrial inhibitors: a unified hypothesis of how cannabinoids modulate mitochondrial function and induce cell death, Biochem. Biophys. Res. Commun. 364 (2007) 131–137.
[27] P. Zaccagnino, S. D'Oria, L.L. Romano, et al., The endocannabinoid 2-arachidonoylglicerol decreases calcium induced cytochrome c release from liver mitochondria, J. Bioenerg. Biomembr. 44 (2012) 273–280.
[28] C. Lipina, K. Macrae, T. Suhm, et al., Mitochondrial substrate availability and its role in lipid-induced insulin resistance and proinflammatory signaling in skeletal muscle, Diabetes 62 (2013) 3426–3436.
[29] M. Perez-Carreras, P. Del Hoyo, M.A. Martin, et al., Defective hepatic mitochondrial respiratory chain in patients with nonalcoholic steatohepatitis, Hepatology 38 (2003) 999–1007.
[30] G. Vial, H. Dubouchaud, K. Couturier, et al., Effects of a high-fat diet on energy metabolism and ROS production in rat liver, J. Hepatol. 54 (2011) 348–356.
[31] J.A. Baur, K.J. Pearson, N.L. Price, et al., Resveratrol improves health and survival of mice on a high-calorie diet, Nature 444 (2006) 337–342.